Ionics (2009) 15:513–518
DOI 10.1007/s11581-008-0299-8

SHORT COMMUNICATION

Optical properties of glasses in the Li_2O–MoO_3–P_2O_5 system

M. Azmoonfar · M. H. Hekmat-Shoar · M. Mirzayi · H. behzad

Received: 12 July 2008 / Revised: 19 October 2008 / Accepted: 13 November 2008 / Published online: 4 December 2008

Abstract Glasses $x$$Li_2O$–(50-$x$)$(MoO_3)_2$–50$P_2O_5$ with x= 10, 20, 30, and 40 mol% were prepared and their optical and electrical properties were investigated. Analysis of the IR spectra revealed that the Li^+ ions act as a glass modifier that enter the glass network by breaking up other linkages and creating non-bridging oxygens in the network. The optical absorption edge of the glasses was measured for specimens in the form of thin blown films and the optical absorption spectra of those were recorded in the range 200–800 nm. From the optical absorption edges studies, the optical band gap (E_{opt}) and the Urbach energy (E_e) values have been evaluated by following the available semi-empirical theories. The linear variation of $(\alpha h\nu)^{1/2}$ with $h\nu$, is taken as evidence of indirect interband transitions. The E_{opt} values were found to decrease with increasing Li_2O content by causing increase in the number of non-bridging oxygens in network. The Urbach tail analysis gives the width of localized states between 0.48 and 0.74 eV.

Keywords Phosphate glasses · IR spectra · Absorption edge · Optical band gap · Urbach energy

Introduction

In the recent years, glasses containing transition metal ions have attracted attention because of their potential applications in electrochemical, electronic, and electro-optical devices. Many glassy materials have been synthesized inside various binary or ternary systems using network forming oxides such as B_2O_3, P_2O_5, and TeO_2 and alkali or silver oxides as network modifiers [1]. In general, the properties of a glass depend upon its composition and to a considerable extent upon its structure [2]. Transition metal oxides (TMO) mixed with P_2O_5 oxide can form homogenous vitreous materials. Conduction for semi-conducting behavior in these glasses is strongly influenced by the simultaneous presence of the transition metal ion in two different valence states in the glass network and conduction can occur by the electron transfer from ions in a lower valence state to those in a higher valence state. The charge transport in these glasses is usually considered in terms of the small polaron hopping theory [3, 4]. Alkali oxides when added to the oxide glasses, act as network modifiers by giving rise to non-bridging oxygens (NBOs) in the structure. The modifiers induce defects and further doping has been found to have a profound effect on a number of physical and chemical properties of glasses [3, 5, 7]. It is expected that in TMO glasses containing modifier ions, a mixture of ionic and polaronic conduction will exist [8]. Purely ionic conducting glasses can be used as solid electrolytes and those exhibiting mixed electronic–ionic conduction can be employed as cathode materials in novel electrochemical cells [8, 9].

The optical absorption coefficient $\alpha(\omega)$ of amorphous semiconductors increases with photon energy in the range of $1<\alpha(\omega)<10^4$ cm^{-1} [26]. In many amorphous semiconductors and dielectrics, the variation of the absorption coefficient with photon energy shows three regions. The first is the region of very high absorption, the second extends over several orders of magnitude of $\alpha(\omega)$ and the third is described as a weak absorption tail. For the higher

M. Azmoonfar · M. H. Hekmat-Shoar (✉) · M. Mirzayi · H. behzad
Physics Department, Sahand University of Technology, Tabriz, Iran
e-mail: Hekmatshoar@sut.ac.ir

values of the absorption coefficient at the absorption edge, the form of $\alpha(\omega)$ with photon energy was given in quadratic form by Tauc et al. and discussed in more general terms by Mott and Davis whose equation was of the form $\alpha(\omega)\hbar\omega = B\left(\hbar\omega - E_{op}\right)^n$, where B is a constant, E_{op} is the optical gap, and n is an index which usually has the value 2 for amorphous materials, this being the value appropriate to absorption by indirect transitions in k-space. According to the above expression, E_{op} has the value $\hbar\omega$ when the quantity $[\hbar\omega\alpha(\omega)]^{1/2} = 0$ [29]. The other region of the absorption edge at lower values of $\alpha(\omega)$ is often described by a relationship developed by Urbach. He assumed that in this region, the absorption coefficient was an exponential function of the photon energy $\hbar\omega$ and, therefore, $\alpha(\omega) = \alpha_0 \exp(\hbar\omega/E_e)$,where α_0 is a constant and E_e is the Urbach energy [29, 31].

In this work, we report the infrared spectra of $x\mathrm{Li_2O}$–$(50\text{-}x)(\mathrm{MoO_3})_2$–$50\mathrm{P_2O_5}$ with x=10, 20, 30, and 40 mol% glasses in order to elucidate the structures of the glasses. The studied glass compositions help following structural changes in the phosphate matrix due to addition of MoO_3 and/or Li_2O. Optical and electrical properties of the glasses (optical gap and Urbach energy) are investigated to determine the optical transition characteristics and provide information about the band structure and energy gap.

Experimental procedures

Glasses of the Li_2O–MoO_3–P_2O_5 ternary system were obtained by the classical quenching technique, they were prepared by mixing and grinding together appropriate amounts of Li_2CO_3 (Merck, Germany; 99.5%), $NH_4H_2PO_4$ (Scharlau; 99%), and MoO_3 (Merck; 99.5%) before transferring to an alumina crucible. The mixture was heated in an electric furnace first at 650 K for 2 h to remove the volatile products, according to the reactions of the following type:

$$y\mathrm{Li_2CO_3} + 2z\mathrm{MoO_3} + 2x\mathrm{NH_4H_2PO_4} \rightarrow$$

$$\left(y\mathrm{Li_2O} - z(\mathrm{MoO_3})_2 - x\mathrm{P_2O_5}\right) + y\mathrm{Co_2} + 2x\mathrm{NH_3} + 3x\mathrm{H_2O}$$

Then the mixture melted at 1,160 K for 2 h with frequent stirring to ensure homogeneity. The melt was then poured on steel plates preheated at T=550 K to avoid shattering of the quenched samples due to thermal stress.

The amorphous nature of the samples was established by X-ray diffraction (XRD) analysis, using a TW3710 philips X'pert diffractometer. A structureless spectrum should be obtained for an amorphous sample (Fig. 1).

FTIR spectra were recorded with an FTIR spectrometer (UNICAM Matson 1000) in the frequency range 400–4,000 cm^{-1} at room temperature. Pellets were prepared for FTIR measurements by mixing and grinding a small quantity of glass powder (2 mg) (The glass samples were ground in a clean mortar to a fine powder) with KBr powder (100 mg) and then packed into a stainless steel mold in a dry box and compressing the mold containing mixtures to form pellets for measurements.

The optical absorption of the glasses were measured at room temperature for samples in the form of thin blown films having a thickness of about 4 to 6 μm, using a UV/VIS Philips spectrophotometer in the wavelength region of 200–800 nm. The blowing films were prepared by blowing in air from the molten glasses. An alumina tube was dipped into a molten glass which caused the formation of a bead on the end of the tube. By steady blowing, films of roughly constant thickness were prepared.

Results and discussion

Infrared spectra

The amorphous nature of samples was established by XRD analysis and are shown in Fig. 1. FTIR spectra of $x\mathrm{Li_2O}$–$(50\text{-}x)(\mathrm{MoO_3})_2$–$50\mathrm{P_2O_5}$ with x=10, 20, 30, and 40 mol% glasses in the wavenumber range between 400 and 4,000 cm^{-1} are shown in Fig. 2. As can be seen, the bands for some compositions are broad and possibly overlapped. No characteristic absorption bands were found in the range 4,000–1,400 cm^{-1}, only there are two broad bands at 3,450 and 1,650 cm^{-1} and a sharp band at 2,361 cm^{-1}. The broad bands are weak and seem to be related to the small amounts of water trapped in the pellets [10, 11] and the sharp band related to oxygen in air. Therefore, the spectral domain useful for the structural approach concerns the region of 1,400–400 cm^{-1}. Table 1 represents the position of the

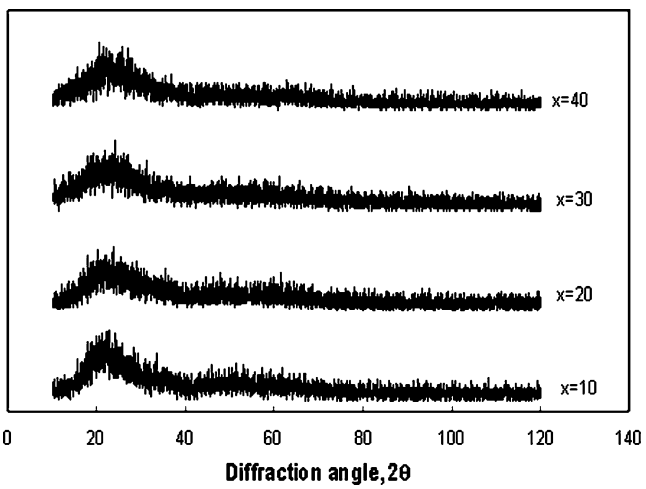

Fig. 1 XRD pattern of the $x\mathrm{Li_2O}$–$(50\text{-}x)(\mathrm{MoO_3})_2$–$50\mathrm{P_2O_5}$ glass system

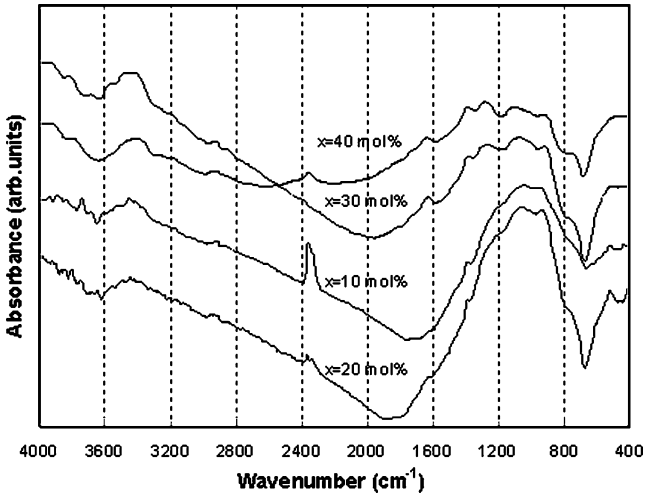

Fig. 2 Infrared absorption spectra of the $x\mathrm{Li_2O}$–$(50\text{-}x)(\mathrm{MoO_3})_2$–$50\mathrm{P_2O_5}$ glass system

absorption bands for the glasses. The bands around 1,383–1,215 cm^{-1} in all the glasses due to stretching vibration of the P=O double bond [2, 10, 12, 14]. The typical IR feature of P_2O_5 glasses are the P=O band at 1,378 cm^{-1} [18]. But when P_2O_5 mixed with other materials there are some differences in position and width of bands.

Other workers have reported a shift of band position when a transition metal oxide such as CuO is added to P_2O_5 glass, with broadening of the band. In amorphous P_2O_5, the glass structure is composed of three bridging oxygen and one P=O that is called ultraphosphate and one feature of this structure is a band at 1,378 cm^{-1}. Also other structures are possible that called meta, pyro, and ortho phosphate. Metaphosphate is composed of two bridging oxygen and two terminal oxygens. Pyrophosphate structure has one bridging oxygen and orthophosphate has not any bridging oxygen [18]. But P=O band, shifts to lower frequency (about 1,260 cm^{-1}) with addition of modifier oxides to compositions. This is because of gradual conversion of ultraphosphate to metaphosphate and pyrophosphate structures [18, 19]. So we can attribute the observed peaks at about 1,383 and 1,260 cm^{-1} to the presence of ultra- and metaphosphate structure in samples.

Table 1 Infrared absorption band positions for $x\mathrm{Li_2O}$–$(50\text{-}x)(\mathrm{MoO_3})_2$–$50\mathrm{P_2O_5}$ glasses

X (mol%)	PO_4^{3-}	P–O–M (M=P, Mo)	MoO_4^{2-}	$P\text{–}O^-$	P=O	H_2O
10	523	795	950	1,060	1,215 1,381	1,640 3,460
20	530	784	938	1,063	1,230 1,384	1,640 3,470
30	530	778	920	1,084	1,284 1,384	1,660 3,450
40	500	775	923	1,100	1,292 1,384	1,661 3,430

These P=O bands shift to a lower frequency as the MoO_3 content increases, the absorption band around 923 cm^{-1} may be related to the Mo–O stretching frequency of (MoO_6) groups [15]. These bands shift to a higher frequency as the MoO_3 content increases. These results suggest that the bonds P=O and Mo–O are transformed into P–O–Mo and Mo–O–Mo bridging bonds when Mo/P ratio increases [1, 16]. The absorption bands near 1,100 and 1,060 cm^{-1} have been related to the $P\text{–}O^-$ stretching frequencies [10, 17, 14]. The absorption bands for $P\text{–}O^-$ groups near 1,060 cm^{-1} obviously shift to a higher frequency as Li_2O replaces MoO_3. As mentioned in "Introduction", in transition metal oxide glasses, conduction relates to the presence of these ions in two different valence state and explained by polarons theory. Also mobile ions can contribute in conduction mechanism with motion in paths. But interactions between polarons and mobile cations exist in mixed conductors [21].

According to Bazan et al. [21], the electrostatic interactions between mobile ions and polarons give rise to direct coupling between electronic and ionic fluxes. This is called the ion–polaron effect resulting in a decrease of the effective mobility.

In the case of the glasses studied here, Li_2O when added to binary system of the glass (MoO_3–P_2O_5), act as network modifiers and the P–O–P, P–O–Mo bonds were broken and non-bridging oxygen atoms appeared in the neighboring of Li^+ cations, resulting in an ionic conductivity of Li^+ cations [1, 15, 16].

According to studies on K_2O–MoO_3–P_2O_5 glasses, there is the absorption bond near 730 cm^{-1} which has been related to ν_{as}(P–O–*M*)(*M*=P, Mo), and decreases with K_2O constant [15]. Thus we can attribute the absorption bands near 795 cm^{-1} to the P–O–*M* (*M*=P, Mo) ring frequency in these glasses and these bands, shift to a lower frequency as Li_2O replaces with MoO_3. Since it is accepted that the former P_2O_5 (equivalent to P–O–P bonds) is an acidic oxide and the electronegativity of phosphorus and molybdenum ions are comparable, it is reasonable to assume that the P–O–M bonds could easily be disrupted by an alkaline medium. These results suggest that the linkages P–O–*M* (*M*=P, Mo) is disrupted by the presence of Li_2O oxide in the glass [15].

This degradation of the network is accompanied with the formation of weak link such as $Li^+...O^-$ bonds and the presence of NBOs in network [1, 15, 16]. The absorption bands around 500 cm^{-1} which appears in all glasses are attributed to a fundamental frequency of the $(PO_4)^{3-}$ group [10, 14, and 17].

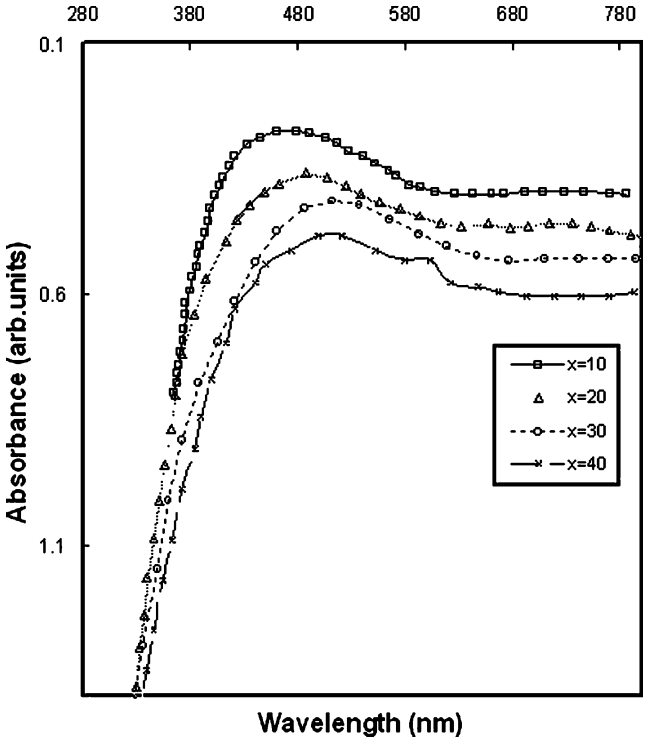

Fig. 3 Optical absorption as a function of wavelength

Table 2 Optical properties of the xLi$_2$O–(50-x)(MoO$_3$)$_2$–50P$_2$O$_5$ glasses

x (mol%)	E_{opt} (eV)	E_e (eV) (λ (nm))	B (cm^{-1} eV^{-1}))
10	2.66	0.48 (373–421)	276.08
20	2.44	0.58 (326–423)	134.32
30	2.16	0.74 (322–487)	111.54
40	2.05	0.67 (355–450)	142.47

Optical absorption edge

The optical band gap and Urbach energy of the glass system are obtained from their ultraviolet absorption edges. The study of optical absorption and particularly the absorption edge is a useful method for the investigation of optically induced transition and for the provision of information about the band structure and energy gap of both crystalline and non-crystalline materials. The optical absorption spectra of the glass samples xLi$_2$O–(50-x)(MoO$_3$)$_2$–50P$_2$O$_5$ with x=10, 20, 30, and 40 mol% as a function of wavelength are shown in Fig. 3. It may be noted that the optical absorption edge is rather less steep compared with those characteristic of mono-crystalline semiconductors, that signifying the glassy nature of the samples. As can be seen, the fundamental absorption edge moves towards the longer wavelengths as the Li$_2$O content is increased. The absorption coefficients $\alpha(\nu)$ are calculated

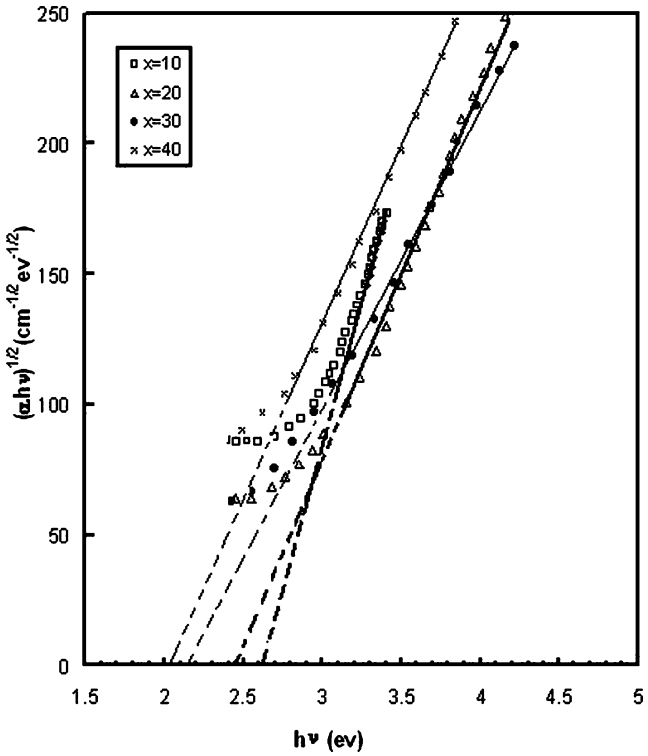

Fig. 4 The $(\alpha h\nu)^{1/2}$ as a function of photon energy ($h\nu$)

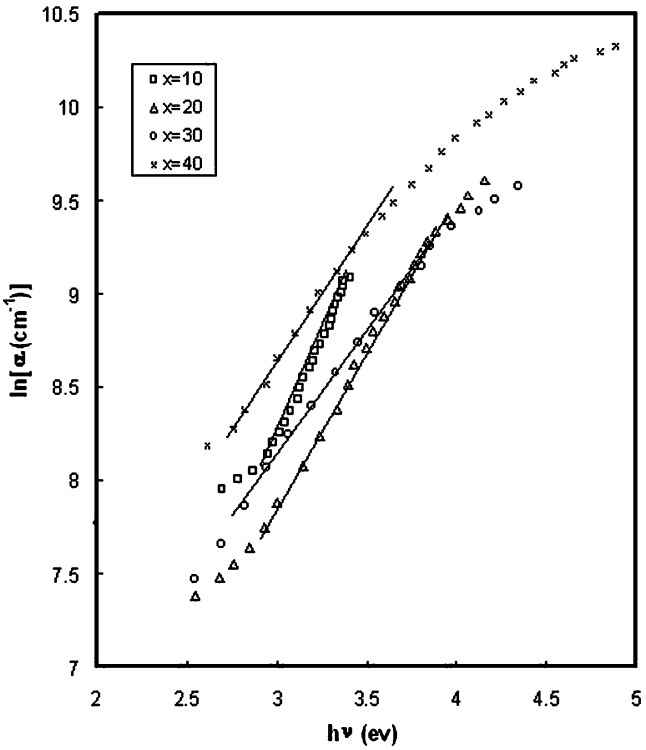

Fig. 5 The ln(α) as a function of photon energy ($h\nu$)

at various wavelength (or frequencies) using the relation [23, 24]:

$$\alpha(\nu) = \frac{2.303}{x} A(\nu) \quad (1)$$

where x is the thickness of the sample and A is absorbance. For the high absorbing region where $\alpha(\nu) \geq 10^{-4}$ cm^{-1}, the optical absorption coefficient follows a power law given by Davis and Mott, which in the most general form is given by:

$$\alpha(\nu) = B \frac{(h\nu - E_{\text{opt}})^n}{h\nu} \quad (2)$$

where n is an index that can have different values depending on the mechanism of interband transitions: 2, 3, 1/2, and 1/3 corresponding to indirect allowed, indirect forbidden, direct allowed, and direct forbidden transitions, respectively. B is a constant called band-tailing parameter, E_{opt} is the optical band gap energy and $h\nu$ is the incident photon energy [22, 23, 25, 26].

Generally, in many glasses, Eq. 2 depicts a straight line response, as shown in Fig. 4, for n=2 and is associated with indirect transitions [20, 27, 28]. The E_{opt} values were determined from the curves representing $(\alpha h\nu)^{1/2}$ as a function of $h\nu$ by extrapolation of the linear region of the plots to $(\alpha h\nu)^{1/2}$=0. Values of E_{opt} and B are listed in Table 2. As can be seen, the optical band gap energy of glasses decreases from 2.66 to 2.05 eV with increasing Li_2O content. The origin of E_{opt} is attributed to photon-assisted indirect transition [5]. Also introduction of Li_2O into the network causes the P–O–P and P–O–Mo bonds to be broken and appearing of the NBOs in the network. Thus, increasing of Li_2O content introduces greater disorder in the glass network and leads to decrease of the E_{opt}. Also, we may say that, the increase in the concentration of Li^+ ions that participate in the depolymerization of the glass network leads to an increase in the concentration of bonding defects and NBOs. This leads to an increase in the degree of localization of electrons thereby increasing the donor centers in the glass matrix. The increasing presence of these donor centers decreases the optical band gap and shifts the absorption edge towards higher wavelength side.

It is known that disordered and amorphous materials produce localized states in the band gap [29], resulting in an exponential absorption tail. For the absorption coefficient $\alpha(\nu) \leq 10^{-4}$ cm^{-1} there is usually an Urbach tail where $\alpha(\nu)$ depends exponentially on the photon energy $h\nu$ as:

$$\alpha(\nu) = \alpha_0 \exp\left(\frac{h\nu}{E_e}\right) \quad (3)$$

where ν is the frequency of the radiation, α_0 is a constant and E_e is the width of the tails of the localized states at the band gap that represents the degree of disorder in amorphous semiconductors [23, 25, 5, 30]. Figure 5 shows the relationship of lnα against $h\nu$. Ee values were estimated from the slopes of the linear portions as shown in Table 2. It is also interesting to observe that the Urbach energy (E_e) increases with increases Li_2O content. The values of E_e estimated for the xLi_2O–(50-x)$(MoO_3)_2$–$50P_2O_5$ glasses are more than that for MoO3–P2O5 glasses which it is in the rang of 0.23 to 0.39 eV depending on glass composition [8]. Therefore addition of Li_2O to the binary glass leads to introduce more disorder in the glasses network and therefore width of the localized state increases. Also wavelength regions that Urbach energy has calculated are summarized in Table 2.

The nature of this exponential tail absorption is not clearly known. Tauc and Menth [25] suggested that it arises from transitions between the localized states in the band edge tails, the density of which is assumed to fall exponentially with energy. Mott and Davis believed this to be unlikely, as the slopes of the observed exponential absorption edges are very much the same, in a large number of materials. Dow and Redfield believe that the spectral Urbach rule is due to the random internal electric field associated with the structural disorder which broadens the exciton line [8, 29].

Conclusions

The spectral analyses of infrared spectra of xLi_2O–(50-x)$(MoO_3)_2$–$50P_2O_5$ glasses revealed that addition of Li_2O to the glass network lead to following results; breakdown of the P–O–M (M=P, Mo) bands and leads to formation of NBOs in the network.

The E_{opt} values for the glasses show a considerable decrease with an increase in Li_2O content. This may be attributed to increase in the number of NBOs as Li_2O introduces greater disorder in the glass network. The width of the tails of the localized states at the band gap (Urbach energy) increases with addition of Li_2O into the MoO_3–P_2O_5 binary system. Also, this can be related to increase of disorder in the MoO_3–P_2O_5 binary glasses network.

References

1. Bih L, El Omari M, Reau JM, Haddad M, Boudlich D, Yacoubi A, Nadiri A (2000) Solid State Ion 132:71–85
2. Subbalakshmi P, Veeraiah N (2002) J Non-Cryst Solids 298:89–98
3. Abbas L, Bih L, Nadiri A, El Amraoui Y, Mezzane D, Elouadi B (2007) J Mol Struct 876:194-198
4. Hekmat-Shoar MH, Hogarth CA, Moridi GR (1985) J Mater Sci 20:889–894
5. Subrahmanyam K, Salagram M (2000) Opt Mater 15:181–186

6. Gahlot PS, Seth VP, Agarwal A, Sanghi S, Chand P, Goyal DR (2005) J Physica B 355:44–53
7. Sambasiva Rao K, Srinivasa Reddy M, Ravi Kumar V, Veeraiah N (2007) Physica B 396:29–40
8. Mansour E, El-Egili K, El-Damrawi G (2007) Physica B 392:221–228
9. Jozwiak P, Garbarczyk JE (2005) Solid State Ion 176:2163–2166
10. Hekmat-Shoar MK, Hogarth CA, Moridi GR (1991) J Mater Sci 26:904–908
11. Boudlich D, Bih L, El Hassane Archidi M, Haddad M, Yacoubi A, Nadiri A, Elouadi B (2002) J Am Ceram Soc 85:623–630
12. Doweidar H, Moustafa YM, El-Egili K, Abbas I (2005) Vibr Spectros 37:91–96
13. Moustafa YM, El-Egili K, Doweidar H, Abbas I (2004) J Physica B 353:82–91
14. Metwalli E, Karabulut M, Sidebottom DL, Morsi MM, Brow RK (2004) J Non-Cryst Solids 344:128–134
15. Abbas L, Bih L, Nadiri A, El Amraoui Y, Khemakhem H, Mezzane D (2007) J Therm Anal Calorim 90:453–458
16. Bih L, El Omari M, Reau JM, Nadiri A, Yacoubi A, Haddad M (2001) Mater Lett 50:308–317
17. Shih PY, Ding JY, Lee SY (2003) Mater Chem Phys 80:391–396
18. Metwalli E, Karabulut M, Sidebottom DL, Morsi MM, Brow RK (2004) J Non-Cryst Solids 344:128–134
19. Chahine A, Et-tabirou M, Elbenaissi M, Haddad M, Pascal JL (2004) J Mater Chem Phys 84:341–347
20. Hekmatshoar MH (1979) Ph.D. thesis, Burnel University, UK
21. Bazan JC, Duffy JA, Ingram MD, Mallace MR (1996) Solid State Ion 469:86–88
22. Arzeian JM, Hogarth CA (1991) J Mater Sci 26:5353–5366
23. Marzouk SY, Elalaily NA, Ezz-Eldin FM, Abd-Allah WM (2006) Physica B 382:340–351
24. Shih PY, Shiu HM (2007) Mater Chem Phys 106:222–226
25. Tauc J, Menth A (1972) J Non-Cryst Solids, North-Holland 8–10:569–585
26. Tauc J (1970) Mat. Res. Bull, Pergamon press 5:721–730
27. Karmakar B, Kundu P, Dwivedi RN (2001) Mater Lett 47:371
28. Shawoosh AS, Kutub AA (1993) J Mater Sci 28:5060
29. Mott NF, Davise EA (1979) Electronic processes in non-crystalline materials, 1th edn. Oxford University, Oxford
30. Sakata H, Kikuchi T, Qiu HH, Shimizu H, Amano M (1999) J Mater Sci, Mater Electron 10:643–648
31. Edirisinghe SP, Hogarth CA (1989) J Mater Sci 8:789–792